PAPER

Check for updates

Template-free synthesis of monolithic carbon xerogels with hierarchical porosity from resorcinol and formaldehyde *via* hydrothermal reaction†

G. Cho, J. Y. Lee [ID] and T. H. Yoon [ID] *

Monolithic carbon xerogels with hierarchical porosity were prepared from resorcinol (R) and formaldehyde (F) *via* a base-catalysed hydrothermal polycondensation reaction, without a template and supercritical drying. First, an aqueous solution of resorcinol, formaldehyde and sodium carbonate was prepared by varying R/W (25–45) and R/C (1–10k) ratios to produce monolithic RF gels. The reaction was carried out in a pressurized Teflon mould at 100 °C for 6 h to give a co-continuous pore structure *via* spinodal decomposition and a tenacious gel to avoid supercritical drying. Next, the RF gels were dried for 42 h at 60 °C and another 6 h at 100 °C to produce RF xerogels without cracks, followed by pyrolysis in a tube furnace at 900 °C for 2 h under N_2 flow, and then activation at 1000 °C for 2, 4 or 6 h under CO_2 flow. Finally, the carbon xerogels were characterized by SEM and N_2 adsorption–desorption measurements. Monolithic RF gels were obtained from all combinations of R/W and R/C, but the gels from R/W = 45 exhibited a co-continuous large-pore structure, providing a specific surface area (SSA) of ~650 m^2 g^{-1}, which increased to 3311 m^2 g^{-1} (for R/C = 10k) at 6 h of CO_2 activation without exhibiting cracks. N_2 isotherms demonstrated that micro- and meso-pores were introduced *via* activation, forming hierarchical porosity in combination with large pores from spinodal decomposition without using a template.

Introduction

Ever since Pekala introduced the base-catalysed polycondensation reaction of resorcinol–formaldehyde,[1] it has been widely studied for the preparation of porous carbon materials (PCM) of particulates,[2] as well as monoliths,[3–7] with the latter being preferred due to easy handling.[8,9] The recent applications of PCM in electrodes for capacitors, batteries or fuel cells,[10] catalyst supports[11] carbon dioxide capture[12] and water purification[13,14] have led to the desirability of hierarchical porosity for higher performance.[15] This can be achieved by forming not only micro- and meso-pores for a high specific surface area (SSA), and thus, high adsorption, but also macro-pores for higher flow efficiency.[16]

School of Materials Science and Engineering, Gwangju Institute of Science and Technology (GIST), 123 Cheomdan-gwagiro (Oryong-dong), Buk-gu, Gwangju 61005, Republic of Korea. E-mail: thyoon@gist.ac.kr

Consequently, a great deal of research has reported the successful preparation of hierarchical porosity *via* hard–soft templates,[17–19] soft–soft templates,[20] special solvents or additives,[21,22] and polymerization-induced spinodal decomposition with soft templates[23–25] or self-assembly.[26] Of these, the last approach seems to be simpler than the others due to the one-step aqueous solution reaction of RF with only soft templates.[15] However, spinodal decomposition provided aggregation of particles, in general, generating small pores between them, rather than co-continuous pore structure *via* interconnection of particles, while the latter is preferred for better performance. Of course, it was successfully achieved from sol–gel process[27] as well as from some other polymers.[28,29] Moreover, this approach generally requires supercritical or freeze drying to retain the pore structure,[2–6] making the PCM expensive.

Recently, Huang and co-workers reported the successful preparation of monolithic PCM with hierarchical porosity from phenol-formaldehyde without supercritical drying.[30] They reported a co-continuous large pore (10–20 μm) structure with interconnected particles *via* polymerization-induced spinodal decomposition, which is possibly due to hydrothermal reaction. The hydrothermal reaction is also believed to generate a tenacious polymer network to make supercritical drying unnecessary, and thus, providing xerogels. However, its specific surface area (SSA) remained low (~620 m^2 g^{-1}) even with the use of soft templates such as F127. Besides, Jia and co-workers also reported on the successful

preparation of monolithic PCM with hierarchical porosity *via* ambient drying with no hydrothermal reaction.[31]

As noted in the literature, however, the SSA can be increased dramatically by activation.[32–35] For example, Baumann[34] reported a SSA of 3125 $m^2 g^{-1}$ *via* 6 h of CO_2 activation for monolithic PCM at 950 °C (*vs.* 463 $m^2 g^{-1}$ before activation), while 2695 $m^2 g^{-1}$ was obtained *via* 2 h of CO_2 activation at 1000 °C (*vs.* 630 $m^2 g^{-1}$).[33] The increase is believed to be due to the micro- and meso-pores introduced by activation.[36] This suggests that it may be possible to obtain hierarchical porosity *via* activation, rather than utilizing a soft template. However, a high degree of activation is also known to enlarge the existing micro- or meso-pores,[37] generating meso- or macro-pores, which could possibly increase flow efficiency but decrease the SSA. Therefore, activation conditions need to be carefully controlled in order to maximize the micro- and meso-pores for high SSA and to minimize the macro-pores to prevent an appreciable decrease in the SSA while still having enough to ensure good flow efficiency.

To this end, longer activation time,[33] higher temperature[34] and/or higher concentration of activation agents[35] were employed to obtain higher SSA. This in turn led to higher degrees of activation, but was also accompanied by high burn off ratios (~80%), which can be problematic at times.[10] However, a maximum pore volume was also reported at ~40% burn off ratio.[37] SEM micrographs from these studies show that the discrepancy can be attributed to different morphologies. The former showed monolithic PCM with small pores arising from highly aggregated carbon particles,[34] requiring a high burn off ratio to obtain not only micro- and meso-pores but also macro- pores for hierarchical porosity *via* activation. In contrast, the latter used an olive stone with large pores of several microns,[38] requiring only an introduction of micro- and meso-pores for hierarchical porosity, and thus, low burn off ratio reported. Therefore, the latter approach appears to be more promising in obtaining monolithic PCM with large pores without supercritical drying, and hierarchical porosity can be subsequently achieved *via* activation.

In this study, therefore, it was attempted to prepare monolithic xerogel PCM with a co-continuous large (~μm) pore structure *via* base-catalysed polycondensation reaction. Resorcinol was chosen over phenol because of its better solubility in water,[39] while R/W (25–45) and R/C (1–10k) ratios were varied to obtain the monolith.[40] Hydrothermal reaction with a Teflon mould was employed to give a co-continuous large pore structure *via* polymerization-induced spinodal decomposition, as well as a tenacious pore structure to avoid supercritical drying.[41–43] A soft template was not used to make the process simple and inexpensive,[44,45] while micro- and meso-pores were introduced by CO_2 activation to afford hierarchical porosity in combination with large pores from spinodal decomposition.[36] The monolithic carbon xerogels obtained were characterized by SEM and N_2 adsorption–desorption measurements.

Experimental

Materials

For monolithic carbon xerogels with co-continuous large pores, resorcinol (R, Aldrich 398047, >99%), formaldehyde (F, Aldrich

252549, 37 wt% in H_2O) and sodium carbonate concentrate (Aldrich 56169, 0.1 M Na_2CO_3) were used as-received.

Preparation of monolithic RF xerogels *via* hydrothermal process

Monolithic RF xerogels were prepared *via* polycondensation hydrothermal reaction[30] from resorcinol and formaldehyde with sodium carbonate (Na_2CO_3) as a catalyst. First, the RF solution was prepared by charging formaldehyde (F) by weight to a glass vial, followed by the addition of distilled water (W, resistivity of 18 MΩ cm *via* Milli-Q Advantage System) and then resorcinol (R).

Loading of R was varied from 2.5, 3.5 or 4.5 g to afford R/W = 25, 35, or 45, respectively, while R/C ratio (molar) was changed from 1000(1k), 2500(2.5k), 5000(5k) or 10 000(10k) at a fixed R/F ratio of 0.5. These values were chosen based on the model proposed by Scherdel and co-workers to afford monolithic RF gels.[41] The total amount of water was controlled to 10 ml, which included the volume from the 37% formaldehyde (MeOH was considered water). After complete dissolution of R, the mixture poured into a Teflon mould with four holes (36 mm in diameter and 40 mm in depth) and an aluminium top plate to prevent the pressure loss during the reaction. The mould was then placed in an air convection oven at 100 °C for 6 h. The temperature was selected based on the previous study[30] to give a co-continuous pore structure *via* polymerization-induced spinodal decomposition, as well as a tenacious polymer network to avoid supercritical drying. Finally, the RF gels were dried for 42 h at 60 °C and for additional 6 h at 100 °C to achieve complete drying without the appearance of cracks.

Pyrolysis and activation of monolithic RF xerogels

RF xerogels (diameter of ~34 mm and thickness of ~15 mm) were subjected to pyrolysis in a tube furnace (MSTF-1100, Myungsung Eng., Korea). The furnace was heated from RT to 900 °C at 5 °C min^{-1} under N_2 flow of 200 sccm and held for 2 h, before cooling it naturally under N_2 flow. The carbon gels obtained were cut in half and subjected to activation in the same tube furnace, but at 1000 °C under CO_2 flow of 200 sccm for 2, 4 or 6 h. The burn off ratios and crack generation were recorded for comparison. All monolithic carbon xerogels were analysed by SEM (Jeol, JSM-7500F) at 10 keV with carbon coating. Pore characteristics of the monolithic carbon xerogels were measured with an adsorption instrument (ASAP-2010, Micromeritics, USA) using nitrogen at 77 K. Specific surface area (SSA) and pore size distribution were calculated by Brunauer–Emmett–Teller (BET) and Barrett–Joyner–Halenda (BJH) methods, respectively, while the mean pore size was obtained from 4V/SSA. Total pore volumes were calculated from the total single point adsorption of pores less than 300 nm radius at P/P_o = 0.99, and micro-pore volumes were obtained *via* the *t*-plot theory.

Results and discussion

Preparation of monolithic RF xerogels

As expected from the model by Scherdel and co-workers,[41] monolithic RF gels were successfully prepared from all

combination of high R/W (25, 35, and 45) and R/C ratios (1, 2.5, 5, and 10k). Subsequent drying for 42 h at 60 °C and for additional 6 h at 100 °C resulted in disk-shaped RF xerogels without cracks (Fig. S1†). As these were dried under ambient conditions, a much longer time was required, but drying at higher temperatures than 60 °C resulted in the appearance of cracks despite the shorter drying time. The successful preparation of xerogels can be attributed to the hydrothermal reaction using a Teflon mould at 100 °C,[30] which provided tenacious RF gels capable of withstanding drying at 60 °C. A small shrinkage upon drying was observed, making it easy to remove the RF xerogel from the mould. Also, the xerogels were rigid enough to prevent breakage by hand, possibly due to good connectivity or particles.[46]

Pyrolysis of monolithic RF xerogels

When RF xerogels were subjected to pyrolysis, carbon xerogels were generated without a shape change, but a weight loss of ~50% occurred, which was similar to what was reported in a previous study[41] and which was supported by TGA results in this study (Fig. S2†). The loss was also accompanied by a volume shrinkage of ~55%, which can be compared with 50% (ref. 6) and 70% (ref. 46) reported in the literature. The difference can be attributed to the different formulations used. Despite such a loss, the carbon xerogels were still hard enough to withstand hand breakage.

The SEM analysis showed that RF xerogels from R/W = 45 exhibited a co-continuous pore structure with interconnected carbon particles, which is clearly observed in R/W = 45 and R/C = 10k (named as 45-10k) with a pore size of 2–3 μm (Fig. 1). However, there was an increased aggregation of particles as the R/C decreased, resulting in a pore structure with aggregated carbon particles, rather than a co-continuous pore structure (45-1k). It should be noted that the co-continuous pore structure observed from 45-10k was similar to that reported by Baumann and co-workers,[34] which was obtained after carrying out activation for 6 h at 950 °C with CO_2. But the pore size (2–3 μm) observed in our study was much smaller than that observed by Huang and co-workers (10–20 μm),[30] possibly due to the high R/W used in this study. This demonstrated successful preparation of monolithic carbon xerogels with a co-continuous large pore structure from resorcinol and formaldehyde *via* hydrothermal polycondensation reaction.

The gels from R/W = 35 exhibited a pore structure with highly aggregated large carbon particles (~2 μm in diameter) for all R/C ratios, rather than an interconnected co-continuous pore structure (Fig. S3†). A similar pore structure was also observed from R/W = 25, but with a larger particle size (~3 μm), again irrespective of the R/C ratio (Fig. S4†). This demonstrated that the particle size increased with decreasing R/W, as reported previously.[5,6] The effect of R/C ratio on the particle size proved to be negligible in R/W = 25 and 35 gels, but the effect was clearly observed in R/W = 45 gels. This demonstrated that a co-continuous pore structure with interconnected particles can be obtained only if the conditions are optimal, even if polymerization-induced spinodal decomposition is obtained *via* polycondensation hydrothermal reaction.

A N_2 adsorption–desorption study on the R/W = 45 gels, whose co-continuous pore structure was verified, showed either Type I (45-10k, and 45-5k) or Type IV isotherms (45-1k and 45-2.5k), as shown in Fig. 2a. Type I isotherms can be attributed to mostly micro-pores, while Type IV isotherms are attributed to the presence of some number of meso- and macro-pores. This was supported by the pore size distribution measurements (Fig. 2b), which showed a negligible number of meso- and macro-pores for 45-10k and 45-5k, but an appreciable number for 45-2.5k. However, 45-1k exhibited a much higher number of meso-pores but a lower number of macro-pores than 45-2.5k (Fig. 2b). By correlating these with the SEM results (Fig. 1), it can be proposed that as the R/C ratio decreases, the particle size decreases along with increased aggregation, resulting in a larger number of smaller pores such as meso and macro-pores. The decreased number of macro-pores for 45-1k can be attributed to very small particles that can only form meso-pores upon aggregation. This was also supported by the increased mean pore size with lower R/C ratios (Table 1). In addition, the peak at 3–4 nm is believed to be due to the tensile strength effect caused by the ink-bottle or cylinder-type pores.[47]

Furthermore, the calculated total and micro-pore volumes also supported this hypothesis (Table 1), showing an increased total pore volume with lower R/C ratios, but a similar micro-pore volume, irrespective of R/C ratios. The former can be again attributed to the increased meso- and macro-pores due to the decreased particle size and increased aggregation. The latter can be explained by the same amount of resorcinol and formaldehyde used for RF gels, despite their dissimilar morphologies in the SEM, resulting in the same or similar volume and possibly generating a similar amount of micro-pores upon pyrolysis.[46] This was supported by the 50% weight loss upon pyrolysis, irrespective of the R/C ratios, and by the results reported by Yamamoto and co-workers.[6] As expected, similar SSAs of 673, 682, 696, and 656 were obtained for 45-1k, 45-2.5k, 45-5k and 45-10k, respectively.
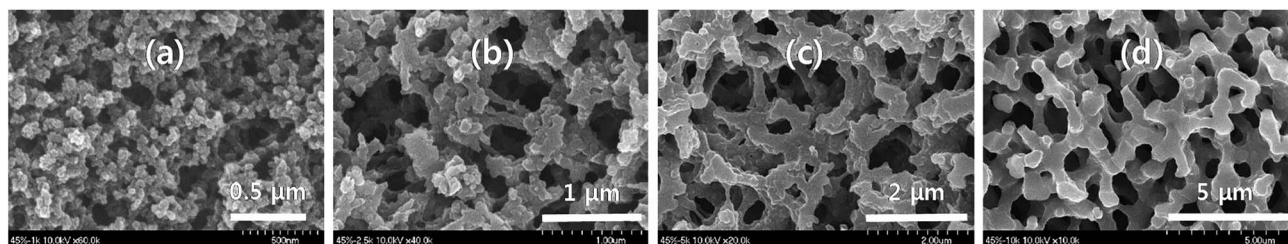

Fig. 1 SEM of RF-based monolithic carbon xerogels, (a) 45-1k, (b) 45-2.5k, (c) 45-5k and (d) 45-10k.
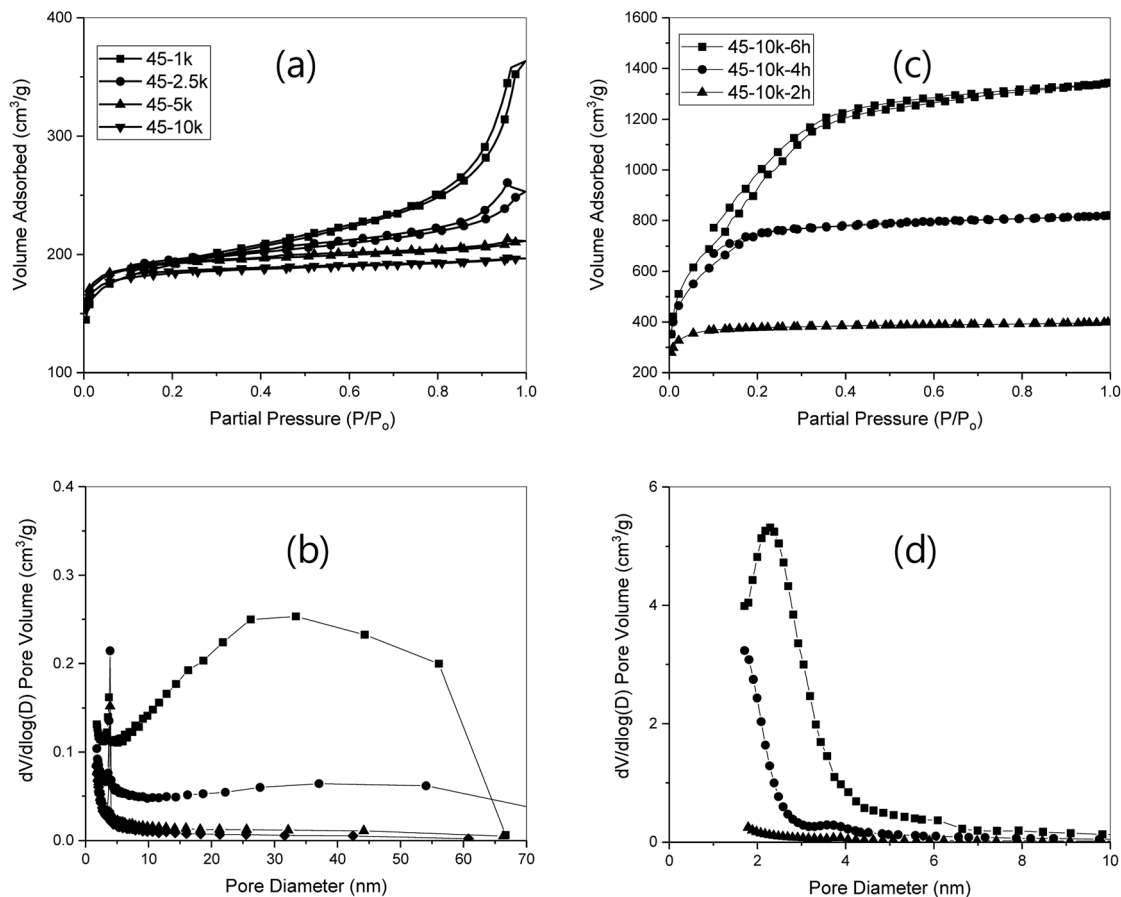
Fig. 2 N$_2$ isotherms of monolithic carbon xerogels from 45-1, 2.5, 5, or 10k (a) and their pore size distribution, (b) isotherms from 45-10k-2 h, 4 h, or 6 h CO$_2$ activation (c) and their pore size distribution (d).

CO$_2$ activation of carbon xerogels

Given that the SSA values of monolithic carbon xerogels from R/W = 45 were very high, activation was carried out under CO$_2$ flow. As expected from a previous study,[34] the longer activation time resulted in higher burn off ratios; for example, 31, 56, or 81% with 2, 4 or 6 h of activation for 45-10k (Table 1). Similar results were obtained from other samples (45-1k, 45-2.5k, or 45-5k), but slightly increased values were observed with lower R/C ratios (Table S1†). Tsuchiya,[33] however, reported increased burn off ratios with higher R/C ratios, which may be explained by the lower catalyst concentration (R/C = 1–10k) and higher reaction temperature (100 °C) used in the study.

Some samples also exhibited a crack or cracks, especially with lower R/C ratios and longer activation time (Table S1†). As noted, large cracks can be correlated to the high burn off ratio. However, the gels from 45-10k did not exhibit any cracks despite the high burn off ratio (as high as 81%) and maintained the monolithic structure, while a slight size reduction was observed in the gels with 6 h of activation. Nevertheless, these gels (45-10k) still provided sufficiently high stiffness even after 6 h of activation to withstand hand breakage. Therefore, these gels were subjected to N$_2$ adsorption–desorption measurements, which provided SSAs of 1306, 2463 and 3311 m^2 g^{-1} for 45-10k-2 h, 45-10k-4 h and 45-10k-6 h, respectively. Given that the

Table 1 Characteristics of monolithic carbon xerogels without and with activation

	S^a (m^2 g^{-1})	V_{total}^b (cm^3 g^{-1})	V_{micro}^c (cm^3 g^{-1})	D_p^d (nm)	BOR^e (%)
45-1k	663	0.516	0.221	2.91	—
45-2.5k	672	0.339	0.237	1.99	—
45-5k	686	0.291	0.256	1.62	—
45-10k	656	0.266	0.246	1.56	—
45-10k-2 h	1306	0.511	0.493	1.56	31
45-10k-4 h	2463	1.049	0.910	1.70	56
45-10k-6 h	3311	1.719	1.359	2.07	81

^{a} Specific surface area. ^{b} Total pore volume. ^{c} Micro pore volume. ^{d} Mean pore size. ^{e} Burn off ratio from weight loss.

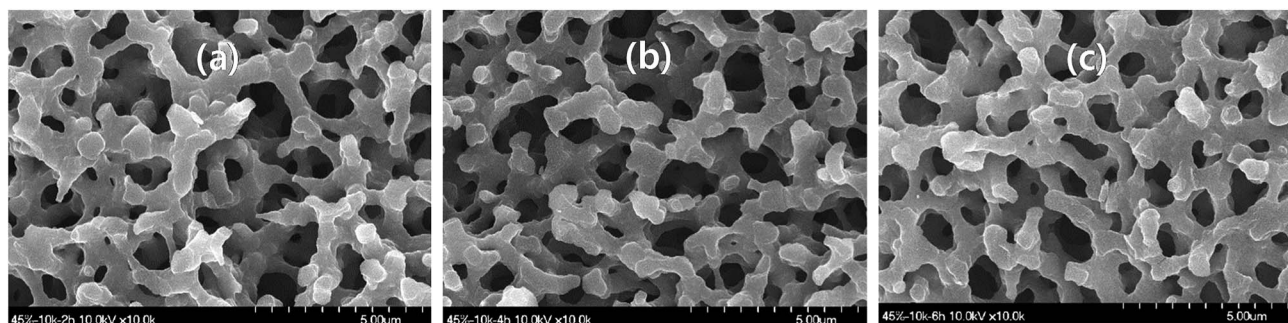**Fig. 3** SEM of activated carbon xerogels from 45-10k for (a) 2 h, (b) 4 h or (c) 6 h activation.

carbon xerogels have a SSA of ∼650 m^2 g^{-1} (before activation), this is a dramatic increase, as expected from earlier studies.[34,43] Type I isotherms were observed from all samples, indicating a presence of mostly micro-pores (Fig. 2c), but adsorption increased highly with longer activation time, demonstrating the introduction of micro-pores, as well as meso-pores, *via* activation. This was supported by the pore size distribution (Fig. 2d), which showed an increased pore diameter from micro- to meso-pores with longer activation time. It was also supported by the increased mean pore size with longer activation time (Table 1). In addition, a higher meso-pore volume was obtained with longer activation time. This corresponded well with the aim of this study, which was to obtain a hierarchical pore structure by combining these micro- and meso-pores with large pores from spinodal decomposition. Unfortunately, the micro-pore volume was 79% and higher than what was expected, despite the very high degree of activation or very high burn off ratio (81%). This can be correlated to the study by Tsuchiya[33] who reported that introduction of meso- or macro-pores *via* activation is proportionally increased to the number of those already in the gel.

Therefore, the isotherms of the gels from 45-2.5k, which already contained micro-, meso- and macro-pores, were obtained. The results showed SSAs of 1468, 2650 and 3163 for 45-2.5k-2 h, 45-2.5k-4 h, and 45-2.5k-6 h, respectively, which were similar to the values obtained from 45-10k. However, these exhibited a combination of Type I and Type IV isotherms (Fig. S5a†), rather than a Type I isotherm, indicating the presence of meso- as well as macro-pores. Also, a small increase in adsorption was noted at high P/P_o, which increased with longer activation time, indicating more macro-pores upon longer activation time. This suggests a much greater number of meso- and macro-pores after activation, which was also supported by the pore size distribution (Fig. S5b†). These results can again be correlated to the study by Tsuchiya,[33] as discussed in the previous paragraph. Thus, the gels from 45-2.5k appears to be better than those from 45-10k in terms of number of meso- and macro-pores observed, but the former exhibited cracks upon activation even at 2 h and was no longer a monolith.

The xerogels from 45-10k after activation showed a very similar morphology to that before activation despite the high burn off ratio (Fig. 3), being similar to the results from earlier study.[7] This indicates no appreciable external burning of the skeleton, which is contrary to what was expected from the high burn off ratio. Thus, high burn off ratio upon activation can be attributed to introduction of micro- and meso-pores, as well as their enlargement to meso- and macro-pores. This may be the reason for the very high SSA after activation.

Conclusion

Monolithic carbon xerogels with hierarchical porosity were successfully prepared *via* base-catalysed hydrothermal polycondensation reaction from resorcinol and formaldehyde, followed by pyrolysis and activation, without a template and supercritical drying. This success can be attributed to (1) high R/W (45) and R/C (1-10k) ratios leading to a monolithic structure, (2) hydrothermal reaction providing a co-continuous large-pore structure *via* spinodal decomposition, as well as tenacious RF gels to avoid supercritical drying, and (3) introduction of micro- and meso-pores *via* activation to form hierarchical porosity in combination with large pores *via* spinodal decomposition. Upon pyrolysis, all xerogels showed ∼50% weight loss and ∼55% volume shrinkage, but CO_2 activation at 1000 °C resulted in a large weight loss and the presence of cracks, which became severe with longer activation time and/or lower R/C ratio. However, the gels from 45-10k showed no cracks and high stiffness, and provided SSAs of 1,306, 2463 and 3311 m^2 g^{-1} for 45-10k-2 h, 45-10k-4 h and 45-10k-6 h, respectively. These values were much higher than ∼650 m^2 g^{-1} obtained from carbon xerogels (before activation) and can be attributed to micro- and meso-pores introduced by activation, which in turn led to the formation of hierarchical porosity in combination with large pores from spinodal decomposition.

Conflicts of interest

There are no conflicts to declare.

Acknowledgements

Notes and references

1 R. W. Pekala, *J. Mater. Sci.*, 1989, **24**, 3221.
2 X. Lu, R. Caps, J. Fricke, C. T. Alviso and R. W. Pekala, *J. Non-Cryst. Solids*, 1995, **188**, 226.
3 R. W. Pekala, C. T. Alviso, F. M. Kong and S. S. Hulsey, *J. Non-Cryst. Solids*, 1992, **145**, 90.
4 R. Saliger, V. Bock, R. Petricevic, T. Tilloston, S. Geis and J. Fricke, *J. Non-Cryst. Solids*, 1997, **221**, 144.
5 H. Tamon, H. Ishizaka, T. Araki and M. Okazaki, *Carbon*, 1998, **36**, 1257.
6 Y. Yamamoto, T. Nishimura, T. Suzuki and H. Tamon, *J. Non-Cryst. Solids*, 2001, **288**, 46.
7 A. Léonard, S. Blacher, M. Crine and W. Jomaa, *J. Non-Cryst. Solids*, 2008, **354**, 831.
8 Y. Liu, J. Luo, C. Helleu, M. Behr, H. Ba, T. Romero, A. Hébraud, G. Schlatter, O. Ersen, D. S. Su and C. Pham-Huu, *J. Mater. Chem. A*, 2017, **5**, 2151.
9 H. Obersacher and C. G. Huber, *TrAC, Trends Anal. Chem.*, 2002, **21**, 166.
10 Y. Zhai, Y. Dou, D. Zhao, P. F. Fulvio, R. T. Mayes and S. Dai, *Adv. Mater.*, 2011, **23**, 4828.
11 I. Matos, M. Bernardo and I. Fonseca, *Catal. Today*, 2017, **285**, 194.
12 A. H. Lu, G. P. Jao and X. Q. Zhang, *Porous carbons for carbon dioxide capture in Porous Materials for Carbon Capture*, Green Chemistry and Sustainable Technology, Springer-Verlag, Berlin Heidelberg, 2014.
13 B. S. Girgis, A. A. Attia and N. A. Fathy, *Desalination*, 2011, **265**, 169.
14 N. A. Fathy, M. S. Rizk and R. M. S. Awad, *J. Anal. Appl. Pyrolysis*, 2016, **119**, 60.
15 S. Dutta, A. Bhaumik and K. C.-W. Wu, *Energy Environ. Sci.*, 2014, **7**, 3574.
16 X.-Y. Yang, L.-H. Chen, Y. Li, J. C. Rooke, C. Sanchezc and B.-L. Su, *Chem. Soc. Rev.*, 2017, **46**, 481.
17 Y. Deng, C. Liu, T. Yu, F. Liu, F. Zhang, Y. Wan, L. Zhang, C. Wang, B. Tu, P. A. Webley, H. Wang and D. Zhao, *Chem. Mater.*, 2007, **19**, 3271.
18 Y. R. Liang, D. Wu and R. Fu, *Langmuir*, 2009, **25**, 7783.
19 Y. Jiao, S. W. Cho, S. Lee, S. H. Kim, S. Y. Jeon, K. Hur, S. M. Yoon, M.-W. Moon and A. Wang, *Adv. Eng. Mater.*, 2018, **20**, 1700608.
20 S. Valkama, A. Nykänen, H. Kosonen, R. Ramani, F. Tuomisto, P. Engelhardt, G. Brinke, O. Ikkala and J. Ruokolainen, *Adv. Funct. Mater.*, 2007, **17**, 183.
21 G. P. Hao, W. C. Li, S. Wang, G. H. Wang, L. Qi and A. H. Lu, *Carbon*, 2011, **49**, 3762.
22 D. Carriazo, M. C. Gutiérrez, M. L. Ferrer and F. del Monte, *Chem. Mater.*, 2010, **22**, 6146.
23 M. C. Gutierrez, F. Pico, F. Rubio, J. M. Amarilla, F. J. Palomares, M. L. Ferrer, F. del Monte and J. M. Rojo, *J. Mater. Chem.*, 2009, **19**, 1236.
24 C. Liang and S. Dai, *Chem. Mater.*, 2009, **21**, 2115.
25 C. Xue, B. Tu and D. Zhao, *Nano Res.*, 2009, **2**, 242.
26 G. Hasegawa, K. Kanamori, T. Kiyomura, H. Kurata, T. Abe and K. Nakanish, *Chem. Mater.*, 2016, **28**, 3944.
27 A. Feinle, M. S. Elsaeser and N. Huesing, *Chem. Soc. Rev.*, 2016, **45**, 3377.
28 G. Hasegawa, M. Aoki, K. Kanamori, K. Nakanishi, T. Hanada and K. Tadanaga, *J. Mater. Chem.*, 2011, **21**, 2060.
29 S. Xu, J. Li, G. Qiao, H. Wang and T. Lu, *Carbon*, 2009, **47**, 2103.
30 Y. Huang, H. Cai, D. Feng, D. Gu, Y. Deng, B. Tu, H. Wang, P. A. Webley and D. Zhao, *Chem. Commun.*, 2008, 2641.
31 X. Jia, B. Dai, Z. Zhu, J. Wang, W. Qiao, D. Long and L. Ling, *Carbon*, 2016, **108**, 551.
32 J. Xu, A. Wang and T. Zhang, *Carbon*, 2012, **50**, 1807.
33 T. Tsuchiya, T. Mori, S. Iwamura, I. Ogino and S. R. Mukai, *Carbon*, 2014, **76**, 240.
34 T. F. Baumann, M. A. Worsley, T. Y.-J. Han and J. H. Satcher, *J. Non-Cryst. Solids*, 2008, **354**, 3513.
35 A. D. Roberts, J.-S. M. Lee, S. Y. Wong, X. Li and H. Zhang, *J. Mater. Chem. A*, 2017, **5**, 2811.
36 W. M. Qiao, S. H. Yoon and I. Michida, *Energy Fuels*, 2006, **20**, 1680.
37 M. Molina-Sabio, M. T. Gonzalez, F. Rodriguez-Reinoso and A. Sepúlveda-Escribano, *Carbon*, 1996, **34**, 505.
38 T. M. Alslaibi, I. Abustan, M. A. Ahmad and A. A. Foul, *AIChE J.*, 2014, **60**, 237.
39 S. A. Al-Muhtaseb and J. A. Ritter, *Adv. Mater.*, 2003, **15**, 101.
40 C. Lin and J. A. Ritter, *Carbon*, 2000, **38**, 849.
41 C. Scherdel, T. Scherb and G. Reichenauer, *Carbon*, 2009, **47**, 2244.
42 R. Petricevic, M. Glora and J. Fricke, *Carbon*, 2001, **39**, 857.
43 H. Zhou, S. Xu, H. Su, M. Wang, W. Qiao, L. Ling and D. Long, *Chem. Commun.*, 2013, **49**, 3763.
44 M. Serwar, U. A. Rana, H. M. Siddiqi, S. U. Khan, F. A. Ahmed Ali, A. Al-Fatesh, A. Adomkevicius, J. A. Coca-Clemente, L. Cabo-Fernandez, F. Braga and L. J. Hardwick, *RSC Adv.*, 2017, **7**, 54626.
45 H. Sun, W. He, C. Zong and L. Lu, *ACS Appl. Mater. Interfaces*, 2013, **5**, 2261.
46 R. W. Pekala, C. T. Alviso, X. Lu, J. Gross and J. Fricke, *J. Non-Cryst. Solids*, 1995, **188**, 34.
47 J. C. Groen, L. A. A. Peffer and J. Perez-Ramirez, *Microporous Mesoporous Mater.*, 2003, **60**, 1.